

Results of the Hydrodynamics Approach to Heavy Ion Collisions

Pasi Huovinen^a

^aSchool of Physics and Astronomy, University of Minnesota
Minneapolis, MN 55455, USA

Recent hydrodynamical calculations for Au+Au collisions at $\sqrt{s_{NN}} = 130$ GeV energy are reviewed, and the initial conditions of hydrodynamical evolution necessary to reproduce experimental data are discussed.

1. Introduction

One of the first measurements at RHIC was the elliptic anisotropy of the particles produced [1]. It was found to be as large as the hydrodynamical prediction [2] and subsequent hydrodynamical calculations achieved good fits to its centrality and p_T dependence [3,4,5]. In the following I review how well hydrodynamical models can fit the data published after those early papers and what constraints the data has set on the initial state of hydrodynamical evolution.

2. Comparison with the data

As an example of hydrodynamical results, I mostly quote the work of Kolb and Heinz [6]. This is not meant to imply that other calculations are of lesser importance, but rather to emphasize how much of the data can be explained using one set of parameters.

2.1. Transverse momentum spectra

The conventional method to initialize hydrodynamical calculations is to fix the initial densities (energy or entropy and net baryon density) to reproduce the observed particle abundancies and to choose freeze-out temperature to reproduce the observed slopes of the spectra. This approach was also applied in [6] where the initial state was fixed to reproduce the charged particle multiplicity as a function of centrality and the freeze-out temperature was chosen to fit the central collision data. Therefore the good fit to pion and antiproton spectra in the most central collisions shown in the upper left panel of fig. 1 is not surprising. On the other hand, the slope of the spectra as a function of centrality are predictions and, as can be seen, the agreement with data is impressive. For antiprotons the prediction lies within the experimental errors up to $p_T = 3$ GeV/ c . Only for very peripheral collisions, $b > 10$ fm, do the data show a significant excess of particles at $p_T > 1.5$ GeV/ c . In hydrodynamical description the observed excess of antiprotons over pions at $p_T \gtrsim 2$ GeV/ c is simply a consequence of strong transverse flow.

In this calculation local chemical equilibrium is assumed to hold until kinetic freeze-out. Since the favoured kinetic freeze-out temperature, $T_f = 130$ MeV, is much smaller than

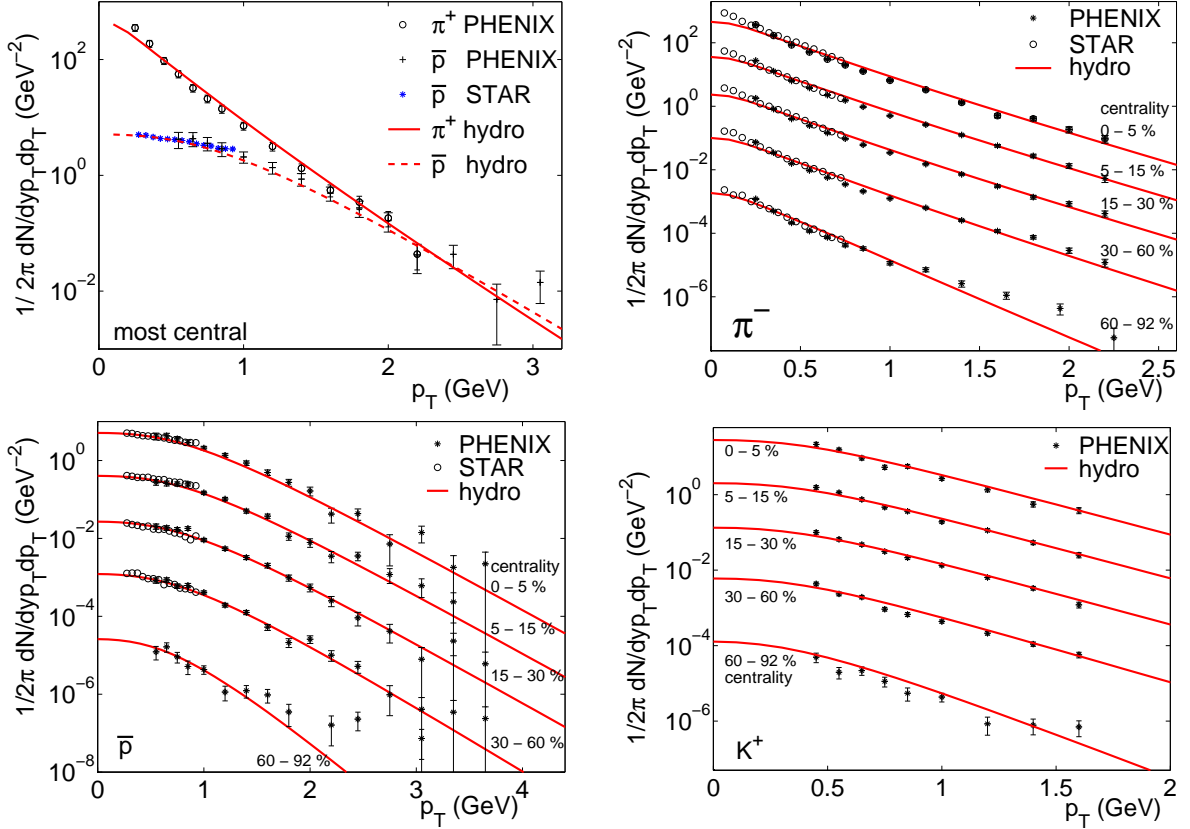


Figure 1. Charged pion, antiproton and positive kaon spectra from central (upper left panel) and semi-central to peripheral (other panels) collisions from [6]. The data were taken by the PHENIX [8] and STAR [9] collaborations.

the chemical freeze-out temperature, $T_{ch} = 165\text{--}175$ MeV given by thermal models [7], it is not possible to obtain correct proton and antiproton yields simultaneously. In [6] this was circumvented by using pion yields at $T_f = 130$ MeV as they were, but scaling by hand all the other particle yields to their calculated values at hadronization temperature $T_c = 165$ MeV. The results obtained in this way are very similar to those of [5] where the hadronic phase is described by a transport model and separate chemical and kinetic freeze-outs are included. Thus one can consider the results of [6] to be reasonable approximations.

2.2. Elliptic anisotropy

Since the initial particle production is azimuthally symmetric, azimuthal anisotropy of the final particle distributions is a signal of rescatterings among the particles produced. More frequent rescattering can be expected to lead to a larger anisotropy, and since hydrodynamics assumes zero mean free path and thus an infinite scattering rate, it provides an upper limit to observable anisotropies. Anisotropy is quantified by measuring the harmonic coefficients $v_n(y, p_T; b)$ of a Fourier expansion in ϕ_p of the measured hadron spectrum $dN/(dy p_T dp_T d\phi_p)$ [10]. Anisotropy characterized by a non-zero second

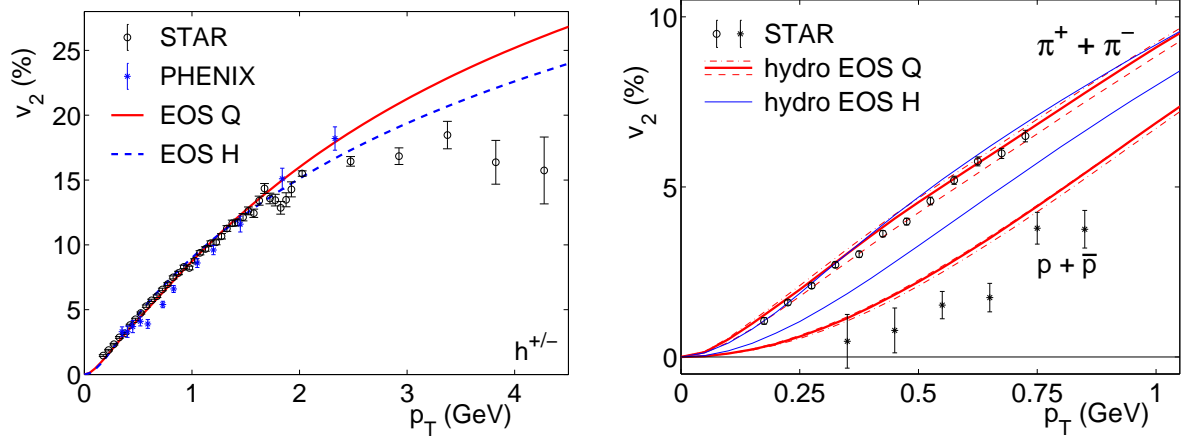


Figure 2. The elliptic anisotropy coefficient $v_2(p_T)$ of all charged particles (left) and identified pions and protons (right) at midrapidity in minimum bias collisions from [6]. The data are from the STAR [1,13,14] and PHENIX [15] collaborations. The curves correspond to calculations using an equation of state with (Q) or without (H) a phase transition and (in the right panel) three different freeze-out temperatures ($T_f = 128$ MeV (dash-dotted), 130 MeV (solid) and 134 MeV (dashed)).

coefficient, v_2 , is called elliptic anisotropy or elliptic flow [11].

The coefficient v_2 as a function of transverse momentum p_T in minimum bias collisions is shown in fig. 2. The calculation was done using an equation of state with a first order phase transition (EOS Q) and without a phase transition (EOS H). The observed anisotropy of charged hadrons shown in the left panel is seen to reach the hydrodynamical values up to $p_T < 2$ GeV. Above $p_T = 2$ GeV the hydrodynamical result keeps increasing monotonically whereas the data saturates, indicating incomplete thermalization of the high momentum particles. The pion and proton anisotropies depicted in the right panel also show the hydrodynamically predicted mass dependence: at low values of transverse momentum, the heavier the particle, the smaller its v_2 [4]. Interestingly at this conference the pion anisotropy was shown to deviate from hydrodynamical predictions around $p_T = 1.5$ – 2 GeV, whereas the proton anisotropy reaches hydrodynamical values even at $p_T \sim 2.5$ GeV [12]. As can be seen the anisotropy of hadrons or pions is quite insensitive to the phase transition, but the anisotropy of protons shows a clear dependence: the curve calculated assuming a phase transition is very close to the data, but an EoS without a phase transition leads to too large a proton anisotropy at low p_T .

The fit to the proton data shown in fig. 2 is worse than achieved in earlier calculations [4, 14]. This is due to a different freeze-out temperature, which was $T_f = 120$ MeV in [4], but was chosen to be $T_f = 130$ MeV in [6] to achieve a better fit to the p_T spectra. On the other hand, the hydro + cascade approach of [5] reproduces well both the p_T spectra and differential anisotropy $v_2(p_T)$ of pions and protons without such ambiguity. Whether this points to a weakness in the ordinary Cooper-Frye description of freeze-out or is a result of differences in the initialization of the calculations remains to be seen.

In fig.3 the centrality dependence of the anisotropy coefficient v_2 is shown. The cal-

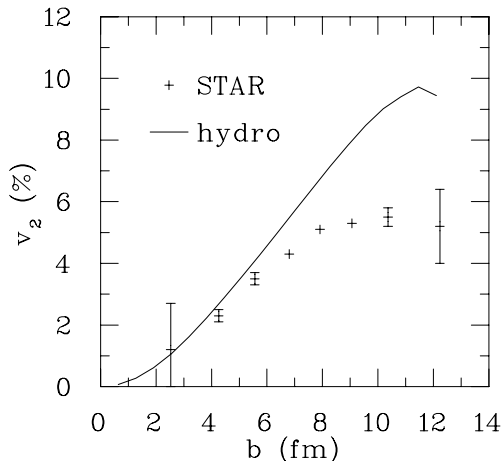


Figure 3. Centrality dependence of elliptic anisotropy of charged particles at midrapidity. The data are analysed using 4th order cumulant method by the STAR collaboration [16].

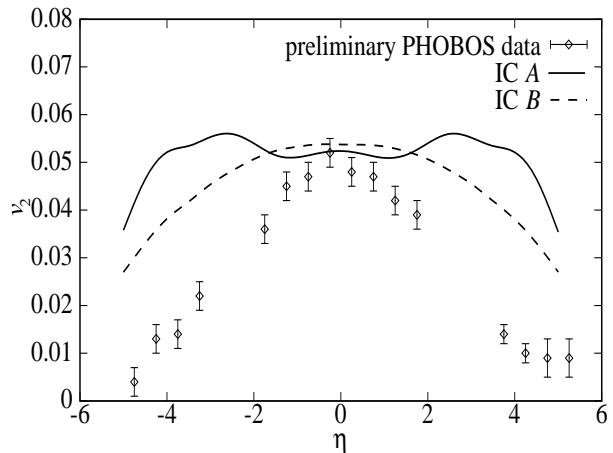


Figure 4. Pseudorapidity dependence of elliptic anisotropy of charged particles in minimum bias collisions from [18]. The preliminary data are from [19]. The curves correspond to two different parametrizations of the initial state.

ulation is similar to that in [6] and the data is analysed by the STAR collaboration [16] using the 4th order cumulant method [17]. The fit to the data is slightly worse than shown before [3] since the 4th order method leads to smaller values of v_2 than previously published [1]. The new values are, however, within the systematic errors of the older analysis. The present data is below the hydrodynamical limit in all but the most central collisions, but the discrepancy is significant only for large impact parameters, $b > 6$ fm.

In the calculations mentioned so far the expansion is assumed to be boost invariant. If the assumption of boost invariance is relaxed and expansion in all three dimensions is done numerically, the centrality and p_T dependence of the anisotropy at midrapidity is similar to that in the boost invariant case [18]. When compared to the excellent fit to data shown in fig. 2, the pseudorapidity dependence of elliptic anisotropy shown in fig. 4 [18] looks less satisfactory. The data reaches the hydrodynamical value only around midrapidity. On the other hand, even this result reproduces the data within a window of one to two units of pseudorapidity. This region already contains most of the particles produced. It is worth remembering that anisotropy in hydrodynamical models depends strongly on the initial shape of the system. The initialization used in [18] is relatively simple and a more sophisticated initialization may lead to better fit to the data. Therefore it is premature to conclude, based on this data and calculation alone, that thermalization is reached only at midrapidity.

2.3. Two-particle interferometry

The analysis of two-particle momentum correlations known as HBT interferometry provides a method to study the space-time structure of the emitting source [20]. It

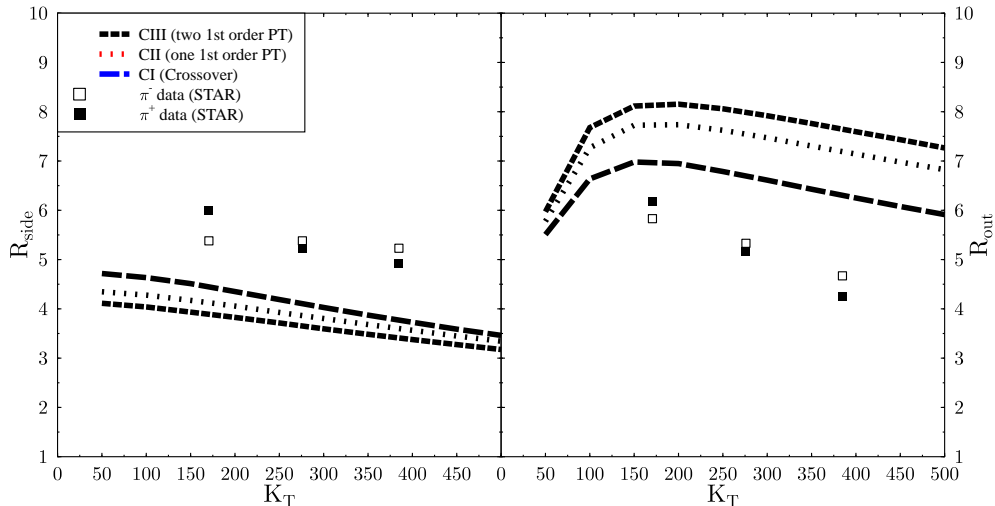


Figure 5. The HBT radii R_{side} and R_{out} from [23]. The data are from [25]. The curves correspond to equations of state with a first order phase transition but different latent heat (CIII and CII) or with a smooth crossover between the phases (CI).

has been predicted that a first order phase transition would lead to unusually large HBT radii [21]. However, comparisons of calculations [6,22,23,24] with data [25,26] have led to the so-called *HBT-puzzle*: All calculations give a ratio of HBT radii $R_{\text{out}}/R_{\text{side}}$ larger than one, but the experimental value is of order one. As shown in fig. 5 [23], hydrodynamics usually leads to a too small sideward radius R_{side} and to a too large outward radius R_{out} . This is usually interpreted to mean that the system expands more and its lifetime is shorter than given by hydrodynamics.

So far it looks like it is possible to fit either R_{side} or R_{out} , but not both simultaneously. A good fit to R_{side} was achieved in [22] where the hadronic phase was described using a hadronic cascade. This naturally leads to a spatial freeze-out distribution with a larger average size in the sideward direction and thus to larger R_{side} . An acceptable fit was achieved also in [24] where the initial size of the system was larger than in other calculations, but the outward radius R_{out} is too large in both of these works. In [6] it was shown that if freeze-out takes place immediately after hadronization, $T_f = T_c = 165$ MeV, R_{out} is reproduced, but R_{side} is even smaller than when the freeze-out temperature is $T_f = 130$ MeV. The effect of such a high freeze-out temperature on single particle spectra or anisotropies was not checked either.

One interesting detail shown in fig. 5 is that the radii are closest to the data when an equation of state with a smooth crossover is used. One can thus claim that HBT radii favour an equation of state with crossover but, as argued above, proton v_2 results favour an equation of state with a first order phase transition. The explanation to this seemingly contradictory behaviour, as well as to the entire HBT-puzzle, is still unknown at present. For the most recent developments see [27].

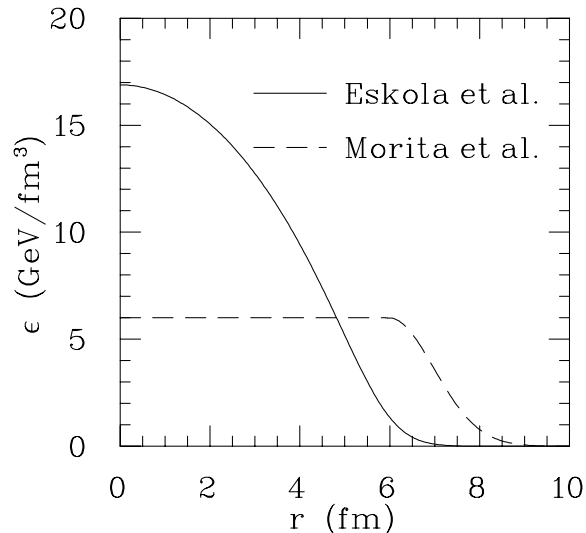


Figure 6. Initial energy density distributions in the transverse plane scaled to $\tau = 1$ fm/c from [24] (Morita *et al.*) and [30] (Eskola *et al.*).

3. Initial conditions

It is well known that even if the hydrodynamical evolution is constrained to reproduce the observed single particle spectra, there still is considerable freedom in choosing the initial state. One degree of freedom which complicates the comparison of the initial state of different hydrodynamical calculations is the initial time, τ_0 , of the calculation. Its effect is easily seen in the Bjorken estimate [28,29] for the initial energy density,

$$\epsilon_{Bj} = \frac{dE_T}{dy} \frac{1}{\tau_0 \pi R^2}, \quad (1)$$

where a smaller initial time leads to a larger initial energy density and vice versa. Thus a meaningful comparison of initial states from different calculations requires scaling the initial densities to the same initial time τ . This is usually done by assuming one dimensional Bjorken expansion with an ideal gas equation of state from the initial time τ_0 of a particular calculation to a chosen common time τ : $\epsilon = \epsilon_0(\tau_0/\tau)^{4/3}$.

However, even if the difference in initial time is taken into account, the final single particle spectra allow very different initial energy distributions. As an example of this, initial energy distributions used in recent calculations by Morita *et al.* [24] and Eskola *et al.* [30] are shown in fig. 6. The former is a simple generalization of the one dimensional Bjorken model to transversely expanding central collisions: a flat energy density distribution with gaussian smearing near the edges. The latter is based on a pQCD saturation calculation [31] of the transverse energy of minijets produced in the primary collisions which leads to a very peaked distribution of energy density. In this approach the net baryon density is also obtained from pQCD calculation and — after fixing the equation of state and equating the initial time with the formation time, $\tau_0 = 1/p_{\text{sat}}$ — the only free parameter is the freeze-out temperature [32].

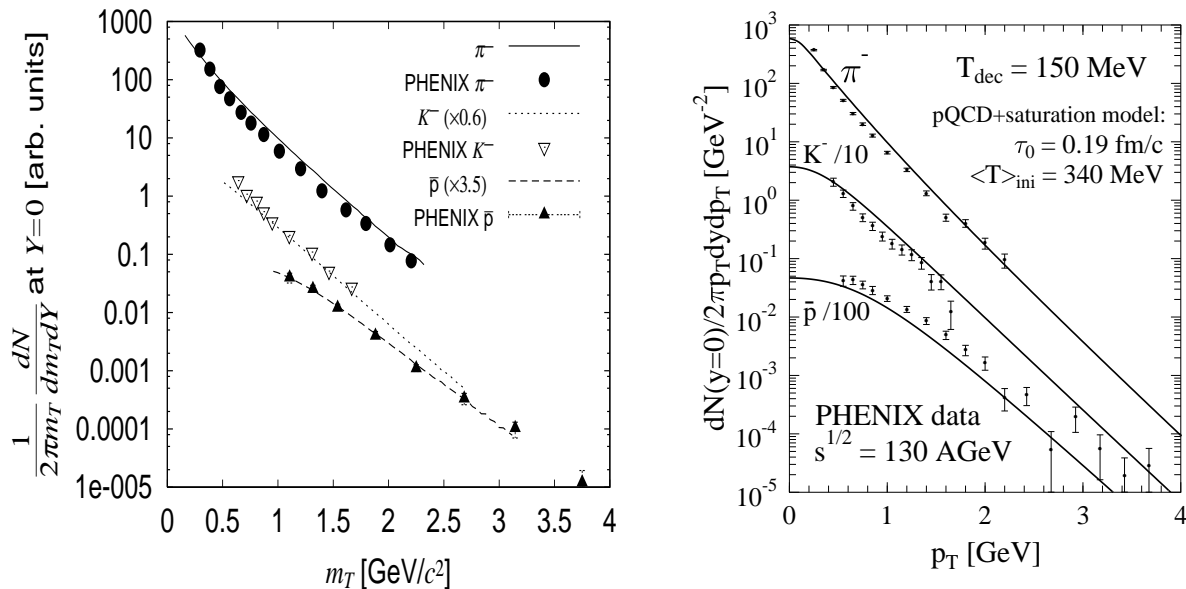


Figure 7. The p_T distributions of negative hadrons calculated by Morita *et al.* [24] (left) and Eskola *et al.* [30] (right) compared to data by PHENIX collaboration [8,33].

Even though the initial states in these two calculations are very different, the final single particle distributions shown in fig. 7 are surprisingly similar and reproduce the slopes equally well! The particle yields must again be treated with caution. In both of these works chemical equilibrium is assumed to hold until kinetic freeze-out. In [24] the kinetic freeze-out temperature $T_f = 125 \text{ MeV}$ is well below the chemical freeze-out temperatures given by thermal models. Thus the authors note that their calculation reproduces the observed slopes of the spectra, but to reach the yields, they must scale them by hand. On the other hand, the authors of [30] employ a considerably high freeze-out temperature, $T_f = 150 \text{ MeV}$, which allows them to reproduce also the particle abundancies.

Unfortunately other observables are not helpful in differentiating these two approaches either. Both of the calculations were done for central collisions where the elliptic anisotropy is zero. The HBT radii are sensitive to the build-up of flow and the lifetime of the system and therefore to the initial distributions, but unfortunately HBT radii were not calculated in [30]. As an estimate one can use the HBT radii for a high freeze-out temperature shown in [6] instead. The radii in [6] and [24] are indeed different, but neither of them reproduces the data: the first leads to a correct R_{out} but too small a R_{side} , whereas the latter reproduces R_{side} acceptably but R_{out} is too large. Another observable which is sensitive to the maximum temperature reached in heavy ion collisions is the spectrum of direct photons, but there is no photon data available yet, nor was the yield calculated in these papers.

Even if the initial energy density distribution is only weakly constrained by the data, the initial energy per unit rapidity is almost fixed. In Table 1 the initial states of recent hydrodynamical calculations are characterized by scaling to $\tau = 1 \text{ fm}/c$ and calculating the average energy density in the transverse plane. The peak values of the initial energy

Table 1

Average initial energy density in the transverse plane scaled to a time $\tau = 1$ fm/ c , initial time, and freeze-out temperature in recent hydrodynamical calculations.

	$\langle\epsilon\rangle(1 \text{ fm}/c)$	τ_0 [fm/ c]	T_f [MeV]
Kolb & Heinz [6]	5.4 GeV/fm ³	0.6	130
Hirano [18]	5.8 GeV/fm ³	0.6	137
Teaney <i>et al.</i> [5]	~ 6 GeV/fm ³	1.0	N/A
Morita <i>et al.</i> [24]	3.9 GeV/fm ³	1.0	125
Eskola <i>et al.</i> [30]	6.5 GeV/fm ³	0.19	150–160

density have a huge spread from 6 to 160 GeV/fm³ in these works, but the average values at 1 fm/ c have a much smaller spread from 3.9 to 6.5 GeV/fm³. This spread is partially due to the different values of the effective transverse area, πR^2 . If this is taken into account, the average energy density in all works is 5–6 GeV/fm³, very similar to the the Bjorken estimate 4.6 GeV/fm³ [29].

The initial times of hydrodynamic evolution employed in these calculations have a relatively large spread from 0.2 to 1 fm/ c . However, in all calculations the initial time is shorter than the perturbatively estimated thermalization time of a few fm/ c [34]. The basic argument in favour of a short initial time is based on elliptic anisotropy; the estimate by Kolb *et al.* [2] showed that if there is 1 or 2 fm/ c delay in thermalization, the value of v_2 decreases by 10% or 25 %, respectively, which leads to values of v_2 which are below the data.

There is no similar consensus about the freeze-out temperature at RHIC. The single particle spectra in central collisions can be fitted equally well (fig. 7) if freeze-out takes place almost immediately after hadronization at $T_f = 150$ –160 MeV [30] or at $T_f = 125$ MeV [24], roughly at the same temperature as at the SPS. The elliptic anisotropy of protons provides an additional constraint on the freeze-out temperature. So far it seems to favour a relatively low freeze-out temperature of $T_f \leq 130$ MeV, but whether it is possible to fit the elliptic anisotropy data using same kind of initial state and freeze-out temperature as in [30] remains to be seen. While discussing freeze-out temperature at RHIC it is also worth remembering that in the hybrid model of [5], where the plasma phase is described using hydrodynamics and the hadron phase using hadronic cascade (RQMD), freeze-out temperature is not well defined.

4. Summary

Hydrodynamical models have been very successful in explaining the single particle RHIC data at low p_T . The p_T spectra and anisotropies in central and semicentral collisions are well reproduced for $p_T \leq 1.5 - 2$ GeV, and the \bar{p}/π ratio at $p_T \sim 2$ GeV/ c has a simple explanation due to flow. Especially impressive has been how hydrodynamics is able to create simultaneously an elliptic anisotropy of negative hadrons which is large enough and an anisotropy of protons which is small enough to fit the data. If one considers solely this data the collision system behaves like a thermal system.

However, the reproduction of the HBT radii has been unsuccessful so far. It is unclear whether one should refine the final freeze-out process, the hadronization process, or the initial state to reach an acceptable description of the data. Especially puzzling is the fact that the HBT radii seem to favour a relatively stiff equation of state with a crossover phase transition, whereas the elliptic anisotropy of protons favours a soft equation of state with a first order phase transition.

The details of the initial state required to fit the data are not yet completely fixed. The common features of all calculations are that the collision system thermalizes rapidly — initial time is $\tau_0 \leq 1 \text{ fm}/c$ — and that the average initial energy density is well above the critical energy density.

Acknowledgements

This work was supported by the US Department of Energy grant DE-FG02-87ER40328.

REFERENCES

1. K. H. Ackermann *et al.* [STAR Collaboration], Phys. Rev. Lett. **86** (2001) 402.
2. P. F. Kolb, J. Sollfrank and U. W. Heinz, Phys. Rev. C **62** (2000) 054909.
3. P. F. Kolb, P. Huovinen, U. W. Heinz and H. Heiselberg, Phys. Lett. B **500** (2001) 232.
4. P. Huovinen, P. F. Kolb, U. W. Heinz, P. V. Ruuskanen and S. A. Voloshin, Phys. Lett. B **503** (2001) 58.
5. D. Teaney, J. Lauret and E. V. Shuryak, nucl-th/0110037;
D. Teaney, private communication.
6. U. W. Heinz and P. F. Kolb, hep-ph/0204061.
7. P. Braun-Munzinger, D. Magestro, K. Redlich and J. Stachel, Phys. Lett. B **518** (2001) 41; W. Florkowski, W. Broniowski and M. Michalec, Acta Phys. Polon. B **33** (2002) 761.
8. J. Velkovska [PHENIX collaboration], Nucl. Phys. A **698** (2002) 507.
9. C. Adler *et al.* [STAR Collaboration], Phys. Rev. Lett. **87** (2001) 262302.
10. S. Voloshin and Y. Zhang, Z. Phys. C **70** (1996) 665.
11. J. Y. Ollitrault, Phys. Rev. D **46** (1992) 229.
12. T. Chujo, these proceedings.
13. C. Adler *et al.* [STAR Collaboration], Phys. Rev. Lett. **87** (2001) 182301.
14. R. J. Snellings [STAR Collaboration], Nucl. Phys. A **698** (2002) 193.
15. R. A. Lacey [PHENIX Collaboration], Nucl. Phys. A **698** (2002) 559.
16. C. Adler *et al.* [STAR Collaboration], Phys. Rev. C **66** (2002) 034904.
17. N. Borghini, P. M. Dinh and J. Y. Ollitrault, Phys. Rev. C **63** (2001) 054906; Phys. Rev. C **64** (2001) 054901.
18. T. Hirano, Phys. Rev. C **65** (2002) 011901.
19. I. C. Park *et al.* [PHOBOS Collaboration], Nucl. Phys. A **698** (2002) 564.
20. U. W. Heinz and B. V. Jacak, Ann. Rev. Nucl. Part. Sci. **49** (1999) 529;
U. A. Wiedemann and U. W. Heinz, Phys. Rept. **319** (1999) 145.
21. D. H. Rischke and M. Gyulassy, Nucl. Phys. A **608** (1996) 479.

22. S. Soff, S. A. Bass and A. Dumitru, Phys. Rev. Lett. **86** (2001) 3981; S. Soff, hep-ph/0202240.
23. D. Zschesche, S. Schramm, H. Stöcker and W. Greiner, Phys. Rev. C **65** (2002) 064902.
24. K. Morita, S. Muroya, C. Nonaka and T. Hirano, nucl-th/0205040; Phys. Rev. C **65** (2002) 061902.
25. C. Adler *et al.* [STAR Collaboration], Phys. Rev. Lett. **87** (2001) 082301.
26. K. Adcox *et al.* [PHENIX Collaboration], Phys. Rev. Lett. **88** (2002) 192302.
27. P. F. Kolb and U. Heinz, these proceedings; S. Soff, these proceedings; S. S. Padula, these proceedings.
28. J. D. Bjorken, Phys. Rev. D **27** (1983) 140.
29. K. Adcox *et al.* [PHENIX Collaboration], Phys. Rev. Lett. **87** (2001) 052301.
30. K. J. Eskola, H. Niemi, P. V. Ruuskanen and S. S. Räsänen, hep-ph/0206230; these proceedings; S. S. Räsänen, private communication.
31. K. J. Eskola, K. Kajantie, P. V. Ruuskanen and K. Tuominen, Nucl. Phys. B **570** (2000) 379.
32. K. J. Eskola, P. V. Ruuskanen, S. S. Räsänen and K. Tuominen, Nucl. Phys. A **696** (2001) 715.
33. K. Adcox *et al.* [PHENIX Collaboration], Phys. Rev. Lett. **88** (2002) 242301
34. J. Serreau, these proceedings; A. H. Mueller, these proceedings and references therein.